

Analytical Models for Quantized Sub-Band Energy Levels and Inversion Charge Centroid of MOS Structures Derived from Asymptotic and WKB Approximations

H. Abebe*, E. Cumberbatch**, H. Morris*** and V. Tyree*

*USC Viterbi School of Engineering, Information Sciences Institute, MOSIS service, Marina del Rey, CA 90292, USA. Tel: (310) 448-8740, Fax: (310) 823-5624, e-mail: abebeh@mosis.org and tyree@mosis.org

**Claremont Graduate University, School of Mathematical Sciences, 710 N College Ave, Claremont, CA 91711, USA. Tel: (909) 607-3369, Fax: (909) 621-8390, e-mail: ellis.cumberbatch@cgu.edu

***Department of Mathematics, San Jose State University, San Jose, CA 95192, USA, morris@math.sjsu.edu

ABSTRACT

Analytical solutions for the coupled Schrödinger and Poisson equations are usually determined using a triangular or a parabolic potential approximation near the silicon/oxide interface [1-3]. The sub-band energy levels and charge centroid results that are determined from the Schrödinger-Poisson solution are used in compact modeling to estimate quantum effects on MOS structures. In this paper we present improved analytical sub band energy levels and charge centroid models derived using asymptotic and WKB approximations from the coupled Schrödinger and Poisson equations [4, 5]. These give good agreement with numerical results, showing improvement over triangular and parabolic potential approximation results at high surface fields.

Keywords: charge centroid, device modeling, MOSFET, quantum effect, sub-band energy

1 INTRODUCTION

One of the approaches used to model quantum effects in a nano-scale MOSFET device is by solving the coupled Schrödinger and Poisson equations. These coupled equations can be solved directly using numerical methods [1, 6, 7]. However, some approximations must be made to get compact analytical models that are needed to increase computational speed for circuit analysis application.

The approximations used for analytical solution usually come in a form of triangular or parabolic electric potential profile near the silicon/oxide interface and give analytical results for the inversion charge centroid and sub-band energy. These analytical models are useful for compact modeling of the MOS device [2, 3, 8]. In this paper we compare the triangular and parabolic approximations with exact asymptotic results, based on the Wentzel-Kramer-Brillouin (WKB) method of solving the Schrödinger

equation [5]. The next section shows the mathematical framework for developing the models.

2 MODEL EQUATIONS AND DERIVATION

Poisson equation:

$$\frac{d^2V}{dx_1^2} = \frac{q}{\epsilon_s}(n - p + N_a) \quad (1)$$

where $n = n_i e^{(V-\phi)/V_{th}}$ and $p = n_i e^{-(V-\phi)/V_{th}}$ are expressions for the classical charge density. The assumption here is that the doping density $N_a \gg N_d$ in the silicon, where N_d and N_a are the donor and acceptor doping densities respectively. The parameter q represents electron charge, ϵ_s semiconductor permittivity, n electron density, p hole density, n_i intrinsic density, $V_{th} = kT/q$, k Boltzmann constant and T temperature.

The boundary conditions consist of the continuity of electric potential and the electric displacement,

$$\epsilon_s dV/dx_1|_{x_1=0} = \epsilon_{ox}(V_s - V_{gs} + V_{fb})/t_{ox}, \quad \text{at the}$$

silicon/oxide interface $x_1 = 0$, where t_{ox} is the oxide thickness, ϵ_{ox} is the oxide permittivity, ϵ_s is permittivity of the silicon, V_{gs} is the gate voltage, V_s is the surface potential and V_{fb} is the flat band voltage. Scaling the coordinate perpendicular to the channel, electrostatic potential, quasi-Fermi potential according to

$$x_1 = xL_d\sqrt{\ln\lambda/\lambda}, \quad (V, \phi) = (w, \varphi)V_{th} \ln \lambda \quad (2)$$

where $\lambda = N_a / n_i$ and $L_d = \sqrt{kT\epsilon_s / n_i q^2}$ is the Debye length, allows equation (1) to be written as

$$\frac{d^2 w}{dx^2} = \frac{1}{\lambda} (e^{(w-\varphi)\ln\lambda} - e^{-(w-\varphi)\ln\lambda}) + 1 \quad (3)$$

In the inversion layer the appropriate scaling is $\tilde{x} = x \ln \lambda$ and the first order asymptotic approximation there gives the Poisson equation in scaled variables as [9]:

$$\frac{d^2 w}{d\tilde{x}^2} = \frac{1}{\lambda(\ln \lambda)^2} e^{(w-\varphi)\ln\lambda}, \quad w(0) = w_s. \quad (4)$$

The solution of (4) is suitably matched to the depletion layer, and applying the boundary condition at $x=0$, gives

$$w(\tilde{x}) = 1 + \varphi + \{\ln(\ln \lambda) + 2 \ln \alpha_0 - 2 \ln(\sinh(\frac{\alpha_0 \tilde{x}}{\sqrt{2}} + \gamma))\} / \ln \lambda \quad (5)$$

$$\text{where } \gamma = \sinh^{-1}(\alpha), \quad \alpha = \alpha_0 \sqrt{\ln \lambda} \lambda^{(1-w_s+\varphi)/2}.$$

The value of α_0 is determined from the transcendental equation,

$$\alpha_0 = \sqrt{2 + \varphi + \frac{\ln(\ln \lambda)}{\ln \lambda} - \frac{1}{\ln \lambda} + \frac{2}{\ln \lambda} [\ln(2\alpha_0) - \gamma]}. \quad (6)$$

An expansion of equation (5) for small \tilde{x} gives

$$w(\tilde{x}) = w_s - f_s \tilde{x} + O(\tilde{x}^2), \quad (7)$$

$$\text{where } f_s = \frac{\sqrt{2}\alpha_0 \coth \gamma}{\ln \lambda}.$$

By approximating energy due to the band offset at the silicon/oxide interface to be qV_s , the triangular potential well approximation at strong inversion gives the potential energy as

$$U(x_1) = -qV + qV_s = qF_s x_1 \quad (8)$$

$$\text{where } F_s = \frac{V_{th} \sqrt{\lambda} (\ln \lambda)^{3/2} f_s}{L_d} \text{ and } V_s = V_{th} w_s \ln \lambda.$$

The energy band offset at the interface forces the potential energy to be zero at $x_1=0$, [6, 7].

Schrödinger equation:

$$\frac{d^2 \psi_j}{dx_1^2} + \frac{2m^*}{\hbar^2} [E_j - U] \psi_j = 0 \quad (9)$$

where ψ_j is the electron wave function with the corresponding energy eigenvalue E_j , \hbar is Planck's constant divided by 2π and m^* is electron effective mass for motion perpendicular to the transistor channel surface. The boundary conditions for the wave function used in this work are: $\psi_j(0) = \psi_j(\infty) = 0$.

The band bending near the silicon/oxide interface at strong inversion confines the carriers to a narrow surface channel and an electron in the semiconductor conduction band is bounded and its energy is quantized. The model used for electron concentration in j^{th} sub-band is,

$$N_j = 0.38 m_e \left(\frac{kT}{\pi \hbar^2} \right) \ln(1 + \exp(E_f - E_j / kT)) \quad (10)$$

where E_f is the Fermi energy, m_e is the electron mass and $j=0, 1, 2$ (in this work only the first three sub-bands are considered to be important).

Substituting the triangular approximation (8) into (9) and solving the eigenvalue problem gives the Airy functions as solutions for the Schrödinger equation with energy eigenvalue

$$E_j = \left(\frac{\hbar^2}{2m^*} \right)^{1/3} \left((3/2)\pi q F_s \left(j + \frac{3}{4} \right) \right)^{2/3}. \quad (11)$$

Stern, [1], pointed out that (11) is a good approximation when the MOS device is at depletion but overestimates the ground state eigenvalues at strong inversion by 6% compared to the exact result. In [3], the energy eigenvalue expression (11) is claimed to be improved using a parabolic potential well and this improvement reduces the values of (11) by a factor of $(3/2)^{2/3}$. The model in [3] gives good comparison with the numerical Schrödinger-Poisson results at strong inversion.

It is also possible to get analytical expressions for the energy eigenvalues and eigenfunctions using the WKB method without using any approximation on the potential given in (5). Let us first rewrite (9) as

$$\varepsilon^2 \frac{d^2 \psi_j}{dz^2} = Q(z) \psi_j \quad (12)$$

$$\text{where } \varepsilon = \hbar / \sqrt{2m^*},$$

$$\begin{aligned}
Q(x_1) &= U(x_1) - E_j \\
&= -2kT \ln(\sinh \gamma) + 2kT \ln(\sinh(c_1 x_1) + \gamma) - E_j, \\
c_1 &= \frac{\alpha_0 \sqrt{\lambda \ln \lambda}}{\sqrt{2L_d}} \text{ and } z = x_1 - x_1^*.
\end{aligned}$$

In this work the turning point x_1^* for the function Q is used as the charge centroid distance that is given in inverse form, $Q(x_1^*) = 0$, and a similar method is used in [3].

The WKB solution of (12) for regions $x_1 \ll (x_1^* - \varepsilon^{2/3})$, $(x_1^* - \varepsilon^{2/3}) \leq x_1 \leq (x_1^* + \varepsilon^{2/3})$ and $x_1 \gg (x_1^* + \varepsilon^{2/3})$ are given in [5] respectively as

$$\psi_j(x_1) = \begin{cases} \frac{A}{\sqrt{k_j(x_1)}} \sin\left[\frac{1}{\varepsilon} \int_z^0 \sqrt{-Q(t)} dt + \pi/4\right] \\ \frac{A\sqrt{\varepsilon\pi}}{(a_1\varepsilon)^{1/6}} Ai(\varepsilon^{-2/3} a_1^{1/3} x_1) \\ \frac{A}{2\sqrt{k_j^*(x_1)}} \exp\left[-\frac{1}{\varepsilon} \int_0^z \sqrt{Q(t)} dt\right] \end{cases} \quad (13)$$

where A is the normalization constant, $Ai(x)$ is the Airy function, and

$$a_1 = \left. \frac{dQ}{dx_1} \right|_{x_1=x_1^*} = 2kTc_1 \coth(c_1 x_1^* + \gamma),$$

$$k_j(x_1) = \sqrt{-\frac{2m^*}{\hbar^2} Q(x_1)},$$

$$k_j^*(x_1) = \sqrt{\frac{2m^*}{\hbar^2} Q(x_1)}.$$

Using (13) and the boundary condition at $x_1=0$ give

$$I = \int_{-x_1^*}^0 \sqrt{-Q(t)} dt = \varepsilon\pi \left(j + \frac{3}{4}\right) \quad (14)$$

An analytical expression for the energy eigenvalues E_j can be determined by solving equation (14). The above integral I can be rewritten using a change of variables:

$$I = \frac{\sqrt{2kT}}{c_1 \coth \gamma} \int_1^{\exp(E_j/2kT)} \frac{\sqrt{\ln(s)}}{s\sqrt{1+u^2}} ds \quad (15)$$

where

$$\begin{aligned}
s &= \exp(-Q(-t + x_1^*)/2kT), \\
u &= \sqrt{s^2 e^{-E_j/kT} (1 - (F_0/F_s)^2) - 1 + (F_0/F_s)^2} < 1, \\
F_0 &= \frac{\sqrt{2\lambda \ln \lambda} V_{th} \alpha_0}{L_d}.
\end{aligned}$$

Using the first term of the expansion

$$\begin{aligned}
1/\sqrt{1+u^2} &= 1 + 1/2 - (F_0/F_s)^2/2 \\
-s^2 e^{-E_j/kT} (1 - (F_0/F_s)^2)/2 + O(u^4),
\end{aligned} \quad (16)$$

equations (14) and (15) give the result (11) for the energy eigenvalues. If we also include the next two terms and solve for the eigenvalue E_j , an improvement over (11) is achieved:

$$E_j = \left(\frac{\hbar^2}{2m^*}\right)^{1/3} \left(\frac{(3/2)\pi q F_s (j + \frac{3}{4})}{(3/2) - \frac{(F_0/F_s)^2}{2}}\right)^{2/3}. \quad (17)$$

3 RESULTS AND COMPARISONS

In this section we present different comparisons of our results with the numerical, triangular and parabolic approximations. In all comparisons below (Figure 1 to 4), the relative doping density is $\lambda=10^7$, and the quasi-Fermi potential ϕ and Fermi energy E_f are considered to be zero.

In Figure 1 we show that using our new approximation (17) to determine the WKB integral I values in (14) gives a better result compare to the triangular approximation at strong inversion region. Figure 2 shows the numerical value of α_0 that is determined from the transcendental equation (6), and α_0 changes somewhat linearly with the surface potential when the surface potential is below about 0.5V. But afterwards it remains constant when the surface potential is greater than 0.5V. The charge centroid distance in Figure 3 is determined from the turning point of Q and averaged over the sub-band energy density N_j , which is given in (10). As expected the triangular approximation loses its accuracy at strong inversion compare to the exact solution. The final Figure 4 shows comparison of (17) with triangular (11) and parabolic, [3], approximations. Our model gives accurate result in both the depletion and inversion operational regions of the device with a smooth transitional region. However, the triangular approximation

is only accurate at depletion, and the parabolic approximation of [3] is good only at strong inversion.

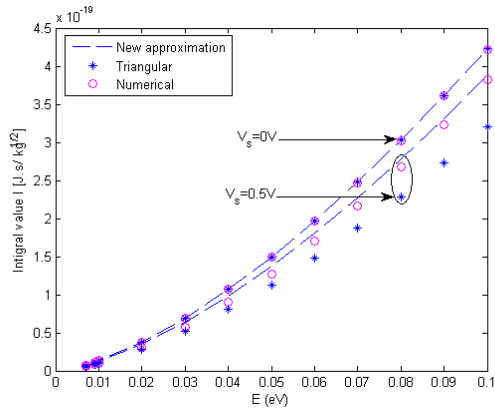


Figure 1: WKB integral, (15), numerical results versus sub-band energy levels compared with the analytical models for different surface potential

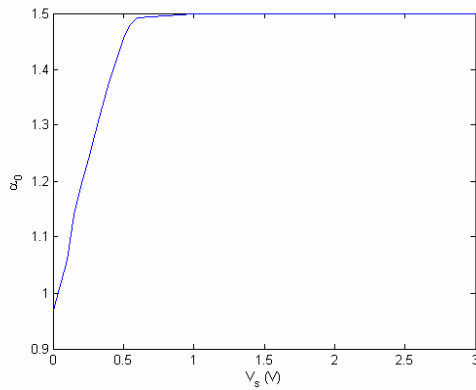


Figure 2: Numerical solution of α_0 from (6) versus surface potential.

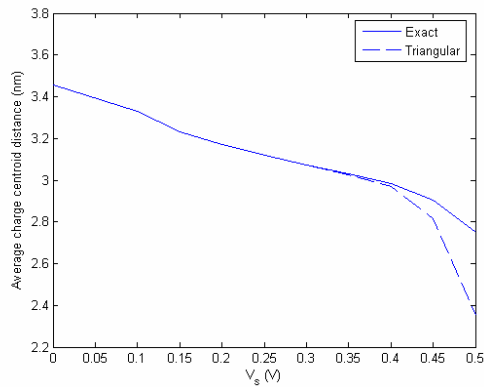


Figure 3: Average inversion layer charge centroid distance as it estimated from the silicon/oxide interface versus surface potential.

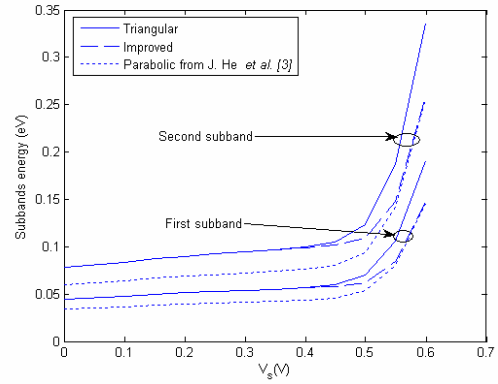


Figure 4: Sub-band energy versus surface potential comparison of different analytical models.

REFERENCES

- [1] M. Stern, "Self-consistent result for n-type Si inversion layers." *Physical Review B*, vol. 5, No. 12, pp. 4891-4899, 15 June 1972.
- [2] H. Abebe, E. Cumberbatch, V. Tyree and H. Morris, "MOSFET analytical inversion charge model with quantum effects using a triangular potential well approximation." *Proceedings 2005 Nanotechnology Conference*, Vol. 3, pp. 64-67, Anaheim, CA, May 8-12, 2005.
- [3] J. He, M. Chan and C. Hu, "A compact model to predict quantized sub-band energy levels and inversion layer centroid of MOSFET with the parabolic potential well approximation," *Proceedings 2005 Nanotechnology Conference*, WCM, pp. 171-174, Anaheim, CA, May 8-12, 2005.
- [4] E. Cumberbatch, H. Abebe, and H. Morris, "Current-voltage characteristics from an asymptotic analysis of the MOSFET equations," *J. of Engineering Mathematics*, vol. 39, pp. 25-46, 2001.
- [5] C. M. Bender and S. A. Orszag, *Advanced mathematical method for scientists and engineers*, McGRAW-HILL, 1978.
- [6] A. Pacelli, "Self-consistent solution of the Schrödinger equation in semiconductor devices by implicit iteration," *IEEE Trans. on Electron Devices*, Vol. 44, No. 7, July 1997.
- [7] S. H. Lo, D. A. Buchanan and Y. Taur, "Modeling and characterization of quantization, polysilicon depletion, and direct tunneling effects in MOSFETs with ultrathin oxides," *IBM J. RES. DEVELOP.* Vol. 43, No. 3, May 1999.
- [8] M. J. Van Dort, P. H. Woerlee and A. J. Walker, "A simple model for quantization effects in heavily-doped silicon MOSFETs at inversion conditions," *Solid State Electronics*, Vol. 37, No. 3, pp. 411-414, 1994.
- [9] M. Ward, F. Odeh, and D. Cohen, "Asymptotic methods for metal oxide semiconductor field effect transistor modeling," *SIAM J APPL. MATH*, vol. 50, No. 4, pp. 1099-1125, August 1990.